RESEARCH ON HEAT AND MASS TRANSFER OF
GAS-WATER
TWO-PHASE FLOW AND THEIR APPLICATIONS

气-水两相流
传热传质及其应用研究

宋保银 编著

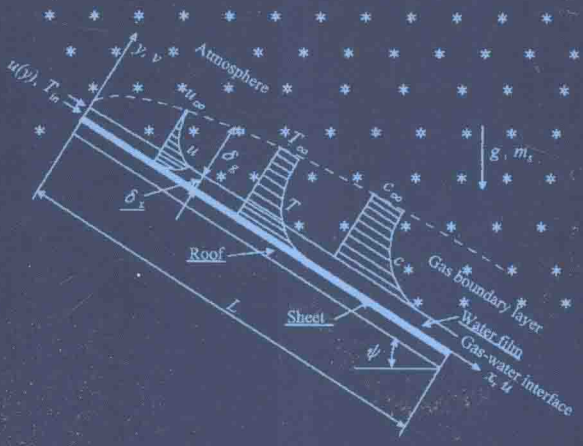

科学出版社

气-水两相流传热传质及其应用研究

Research on Heat and Mass Transfer of Gas-Water Two-Phase Flow and Their Applications

宋保银　编著

科学出版社
北京

内 容 简 介

本书介绍气-水两相流流动、传热与传质及其应用研究。既有机理和特性方面的基础研究，也有其工程应用研究；既有理论分析、数值模拟，也有实验研究。全书内容分为四编：第一编，流下水膜传热传质及其在太阳能热水器、屋顶融雪方面的应用；第二编，动载对气(汽)水两相流流动、传热与传质的影响；第三编，飞行器环境及生命保障工程流动与传热；第四编，双层壁、地下工程、空调及路桥传热。重点阐述太阳照射对流下水膜传热传质影响；动载作用下的气水两相流；座舱及飞行员、人椅系统、飞艇、航天服、月球环境、航天器再入大气层及地面空调与环境工程中的流动和传热。

本书可供能源、动力、机械、土木、传热与传质、制冷、暖通空调、飞行器环境与生命保障、飞行器热控制等领域的学者、科研人员、研究生和工程技术人员参考。

图书在版编目(CIP)数据

气-水两相流传热传质及其应用研究/宋保银编著. —北京：科学出版社，2017.3

ISBN 978-7-03-051963-4

Ⅰ. ①气… Ⅱ. ①宋… Ⅲ. ①气体-液体流动-两相流动-传热传质学-文集 Ⅳ. ①O359-53

中国版本图书馆 CIP 数据核字(2017) 第 042416 号

责任编辑：赵敬伟 / 责任校对：胡庆家
责任印制：张 伟 / 封面设计：耕者工作室

科学出版社出版
北京东黄城根北街 16 号
邮政编码：100717
http://www.sciencep.com

北京中石油彩色印刷有限责任公司 印刷

科学出版社发行 各地新华书店经销

*

2017 年 3 月第 一 版 开本：720 × 1000 1/16
2017 年 3 月第一次印刷 印张：23 1/2
字数：463 000

定价：148.00 元

(如有印装质量问题，我社负责调换)

前　言

传热传质学是近几十年发展起来的一门分支学科，科学技术的发展在不断地充实着它的研究内容和方法。气-水两相流动及其传热传质在自然界、科学和工程领域中经常遇到，像河水流动、汗液蒸发、冷板、水冷却塔、核电站冷却都是很好的例子。作为一门学科，它也为科学技术进步作出了自己的贡献。地球资源的匮乏及地球温暖化，迫使人们对再生能源进行开发和有效利用，冰蓄冷技术及太阳能热水器就是其中两种技术。极端天气的增多，使得自然灾害的频度和损害程度增加，利用温水融雪可以减少积雪对于建筑物的损害。航空航天事业的发展，促进了对于月球环境、飞艇升空、飞行器再入大气层及飞行器环境与生命保障工程传热问题的探讨与研究，也掀起了膜冷却、相变换热、微重力环境及超重力环境下气液两相流及其传热传质研究的热潮。地铁、地下城、高速公路、桥梁的发展，激起了人们对于该工程传热研究的兴趣。

基于以上背景，作者对于气-水两相流传热传质及其应用展开了研究。作者从事传热传质研究和教学三十多年，本书集中反映了作者近二十年的研究成果。全书研究内容共分四部分。第一编，流下水膜传热传质及其在太阳能热水器、屋顶融雪方面的应用。这一部分主要为数值模拟，研究内容包括：流下水膜在辐射加热情况下的热量、质量和动量传递；开式太阳能热水器的能量吸收特性及极限温度和蒸发率；屋顶槽道流下的温水融雪性能及对其预防积雪的数值模拟。第二编，动载对气(汽)水两相流流动、传热与传质的影响。这一部分主要为实验研究，研究内容包括：动载对气水两相流流阻的影响；动载对汽水两相流流动沸腾过程中流型、流阻、传热传质的影响；动载对汽水两相流凝结特性的影响；动载对汽水两相流临界热流密度的影响。第三编，飞行器环境及生命保障工程流动与传热。这部分主要内容包括：飞机风挡和机翼辐射除冰；座舱热环境及飞行员热应激；人椅系统绕流流场数值模拟；飞艇热力性能模拟；航天器乘员舱 CO_2 吸附技术；登月服热力特性；月壤温度计算；航天器再入大气层热力分析。第四编，双层壁、地下工程、空调及路桥传热。这一部分研究内容包括：双层壁玻璃幕墙自然对流换热的数值模拟；地下工程的传热影响因子；

内融冰盘管动态蓄冰特性数值模拟与实验研究；定热流状态下层流和湍流冰浆传热特性；微槽平板热管的流动分析；考虑有风状态下高速路面的热力分析；桥面热性能动态分析。这四个方面研究内容在其他书籍和传热文献中较少涉及，是对传热理论和应用的拓展。考虑到实验成本，选择了气-水两相流传热传质的基础研究，但其研究方法和结果能够较方便地推广到一般的气-液两相流流动及传热传质。本书既强调基础研究，即对现象和机理的揭示，又重视传热理论在居住环境、航空航天领域的实际应用。既有理论分析、数值模拟，也有实验研究。希望书中的实验手段、数学模型、分析方法及研究成果能为读者的研究、工程开发与设计提供参考与借鉴。

本书的研究涉及多人参与、多方支持与资助。首先，感谢与作者合作的同仁：冈山大学的稻叶英男教授（作者的博士生导师）、堀部明彦博士及尾崎公一博士，Patedison 株式会社的高桥敬社长，普渡大学的 R. Viskanta 教授（作者作为访问学者时的联络教授），信州大学的 X. Cao 博士，NEWXT 株式会社的那和克彦部长，中国特种飞行器研究所的周雷研究员，中国飞行试验研究院的于烽高级工程师，南京航空航天大学的曹业玲副教授及袁艳平博士后。其次，感谢为本书研究作出贡献的博士与硕士研究生：姚秋萍、张钊、施红、刘艺涛、李冈 、罗祖分、单绍荣、赵枚、简夕忠、马启成、寇翠翠、毛婷、闫旭东、朱嫣、张宽、王洪、马骞、马良军、张中刚、牟杰、王忠伟、孙中原、徐建峰、宋军辉。第三，感谢国家自然科学基金（50576035）、航空科学基金(03E52027)、高等学校博士学科点专项科研基金（20040287017）对本书研究的经费资助。第四，感谢为本书研究提供实（试）验场所和设施的中国飞行试验研究院、南京航空航天大学、日本冈山大学及美国普渡大学。本书是以论文集的形式编纂的，作者还要感谢刊出这些原始论文的期刊、出版社及论文中引用参考文献的作者。最后作者要感谢科学出版社的合作同仁，通过他们的支持和辛劳，该研究才得以成书，和读者见面。

由于作者的水平限制，书中难免有不足与错误，希望读者与同行不吝赐教，批评指正。另外，本书为中英论文混编，由此给读者带来的不便，也请见谅。

宋保银

于南京航空航天大学

2017 年 2 月

目　录

第一编　流下水膜传热传质及其在太阳能热水器、屋顶融雪方面的应用

这一部分由8篇论文组成，由作者在冈山大学攻读博士学位期间完成，主要为数值模拟，该研究得到Patedison株式会社高桥敬社长的资助及实验验证。研究内容包括：流下水膜在辐射加热情况下的热量、质量和动量传递；开式太阳能热水器的能量吸收特性及极限温度和蒸发率；屋顶槽道流下温水的融雪性能及对其预防积雪的数值模拟。

Heat and Mass Transfer 34 (1999) 387–393 © Springer-Verlag 1999

Heat and mass transfer of a water film falling down a tilted plate with radiant heating and evaporation

B. Song, H. Inaba, A. Horibe, K. Ozaki

Abstract This paper has concerned the heat and mass transfer of a water film falling down a tilted plate with radiant heating and water evaporation. A cluster of physical models was developed for evaluating the properties of heat and mass transfer. A fully implicit control-volume finite-difference procedure was used to solve the coupling equations. The effects of various parameters on heat and mass transfer were investigated. The results showed that the mass fraction of water vapor in ambient atmosphere and the flow turbulence played key roles in the heat and mass transfer. The ambient atmospheric temperature dramatically affected the sensible heat flux. However its effect on the latent heat flux is negligibly small. The magnitude of solar incident flux had an intense influence on the water film temperature.

List of symbols

c	mass fraction of water vapor
c_p	specific heat
D	mass diffusivity
F	local radiation flux
F^o	solar radiation flux incident on the gas-water interface
g	gravitational acceleration
h_{fg}	latent heat of vaporization
h_m	interfacial mass transfer coefficient, $\dot{m}/(\rho_{gI}c_I - \rho_\infty c_\infty)$
h_x	overall interfacial heat transfer coefficient, $q_x/(T_I - T_\infty)$
k	molecular thermal conductivity
$\dot{m}$	interfacial mass flux, $\rho_{gI}v_I$
L	plate reference length
Nu	interfacial Nusselt number, $h_x x/k_g$
p	pressure
Pr_t	turbulent Prandtl number
q_l	interfacial latent heat flux in gas side, $h_{fg}\dot{m}$
q_s	interfacial sensible heat flux in gas side, $-\left[\left(k_g + \frac{\rho_g c_{pg}\epsilon_{Mg}}{\mathrm{Pr}_{tg}}\right)\frac{\partial T_g}{\partial y}\right]_{I,g}$
q_x	total interfacial heat flux, $q_s + q_l$
Re	water film Reynolds number, $4\Gamma/\mu_l$
RH	atmospheric relative humidity
Sc_t	turbulent Schmidt number
Sh	interfacial Sherwood number, $h_m x/D$
T	temperature
u, v	x-direction and y-direction velocities
u_*	shear stress velocity, $(\tau_w/\rho_l)^{1/2}$
x, y	coordinates in axial and transverse directions
X	dimensionless coordinate in the axial direction, x/L
y^+	dimensionless wall coordinate, yu_*/v
y_{um}	the value of y at u reaching the maximum

Greek symbols

α	thermal diffusivity or absorptivity of surface
β	extinction coefficient
λ	wavelength
λ_c	cutoff wavelength beyond which water is opaque to radiation
ρ	density or reflectivity of surface
δ_l	water film thickness
δ_g	thickness of velocity boundary layer of gas
ϵ_M	eddy diffusivity for momentum
μ	dynamic viscosity
ν	kinematic viscosity
τ	shear stress or transmissivity of the gas-water surface
Γ	water mass flow rate per unit width
ψ	tilt angle of the absorbing plate

Subscripts

a	dry air
g	gas mixture of dry air and water vapour
I	condition at the gas-water interface
l	liquid water
v	vapor
w	condition at the absorbing surface
λ	condition at the wavelength of λ
∞	refers to atmosphere

Superscript

$*$	refers to surface radiation property

Received on 29 January 1998

B. Song, H. Inaba, A. Horibe, K. Ozaki
Department of Mechanical Engineering
Okayama University, Okayama 700-0082, Japan

Correspondence to: H. Inaba

The financial support of this work by the Patedison Co. Ltd with Mr. Takashi Takahashi serving as the president is greatly acknowledged. The first author is grateful to the China Flight Test Establishment (Xi'an, China) for supporting him during the course of this study.

1 Introduction

Heat and mass transfer occurs simultaneously in gas- liquid flow systems, which has been studied by numerous investigators [1–6]. Among them, Yan and Soong [1] investigated forced convective heat and mass transfer along an inclined heated plate with film evaporation, and Gandhidasan [4] studied heat and mass transfer in solar regenerators. It is noted that a forced convective [1, 3] or a stagnant [2, 5] gas layer in a gas-liquid flow system is generally focused and a linear distribution of temperature (for laminar flow) or neglecting temperature gradient across liquid film has been suggested by some investigators [4, 6].

The purpose of this study is to determine the heat and mass transfers from a falling water film to an accompanied gas flow, which typically occurs in an open-type flat-plate solar collector, and to investigate the effects of various parameters including the magnitude of the solar radiation, the atmospheric temperature and humidity, the absorbing plate tilt angle and the water film thickness on them. A cluster of physical models had been developed and the characteristics of heat and mass transfer were revealed through solving the related equations numerically.

2 Analysis

The problem concerned in this study is illustrated in Fig. 1. The water falls down a tilted plate as a thin film due to the action of gravity. By the actions of viscous and inertial forces, the ambient gas flows along with the water film forming an accompanying boundary layer. The solar radiative flux incident upon the free surface of the water film is partly transmitted across the film and mainly absorbed by the water film and the absorbing plate which has a high solar absorptivity of surface and is well insulated from back. The heat absorbed by the plate then is transferred to the water film and across it partly to the surrounding gas layer. When evaporation occurs, mass transfer will take place simultaneously between the water film and the gas layer.

Based on "the constant film thickness model" theory [7], assuming a steady two-dimensional turbulent flow and neglecting the gas absorption of the solar radiation, the energy conservation equations for the incompressible water and the accompanying gas, and the concentration equation for gas only reduce to

$$u_l\frac{\partial T_l}{\partial x}+v_l\frac{\partial T_l}{\partial y}=\frac{\partial}{\partial y}\left[\left(\alpha_l+\frac{\epsilon_{Ml}}{\mathrm{Pr}_{tl}}\right)\frac{\partial T_l}{\partial y}\right]+\frac{\partial}{\partial y}\left(\frac{F^+-F^-}{\rho_l c_{pl}}\right) \tag{1}$$

$$\rho_g u_g\frac{\partial T_g}{\partial x}+\rho_g v_g\frac{\partial T_g}{\partial y}=\frac{\partial}{\partial y}\left(\frac{k_g}{c_{pg}}\frac{\partial T_g}{\partial y}\right)+\frac{\partial}{\partial y}\left[\frac{\rho_g T_g D(c_{pv}-c_{pa})}{c_{pg}}\frac{\partial c}{\partial y}\right] \tag{2}$$

and

$$\rho_g u_g\frac{\partial c}{\partial x}+\rho_g v_g\frac{\partial c}{\partial y}=\frac{\partial}{\partial y}\left[\left(\rho_g D+\frac{\rho_g\epsilon_{Mg}}{\mathrm{Sc}_t}\right)\frac{\partial c}{\partial y}\right] \tag{3}$$

where

$$F^+=\int_0^{\lambda_c}F_\lambda^+(y)\,\mathrm{d}\lambda=\int_0^{\lambda_c}\tau_\lambda^* F_\lambda^0 \mathrm{e}^{-\beta_\lambda(\delta_l-y)}\gamma_\lambda\,\mathrm{d}\lambda \tag{4}$$

and

$$F^-=\int_0^{\lambda_c}F_\lambda^-(y)\,\mathrm{d}\lambda=\int_0^{\lambda_c}\rho_{w\lambda}^*\tau_\lambda^* F_\lambda^0 \mathrm{e}^{-\beta_\lambda(\delta_l+y)}\gamma_\lambda\,\mathrm{d}\lambda \tag{5}$$

are the radiative fluxes in the forward (+) and backward (−) directions across the water film thickness (Fig. 2), respectively. In Eqs. (4) and (5)

$$\gamma_\lambda=[1-\rho_{w\lambda}^*\rho_{l\lambda}^*\exp(-2\beta_\lambda\delta_l)]^{-1} \tag{6}$$

is a parameter which accounts for inter-reflection of radiation between the gas-water interface and the absorbing plate surface. ϵ_{Ml} is the water eddy diffusivity for momentum. For $y/y_{um}\le 0.6$, it is evaluated by [8]

$$\frac{\epsilon_{Ml}}{\nu_l}=-0.5+0.5\left\{1+0.64y^{+2}\frac{\tau}{\tau_w}\times\left[1-\exp\left(-\frac{y^+}{25.1}\left(\frac{\tau}{\tau_w}\right)^{\frac{1}{2}}\right)\right]^2 f^2\right\}^{\frac{1}{2}} \tag{7}$$

where $\tau/\tau_w=1-y^+/y_{um}^+$ and $f=\exp(-1.66y^+/y_{um}^+)$ is a damping factor. For $0.6<y/y_{um}\le 1$, the eddy diffusivity is taken as constant and equal to its value at $y/y_{um}=0.6$. ϵ_{Mg} is the eddy diffusivity for momentum of

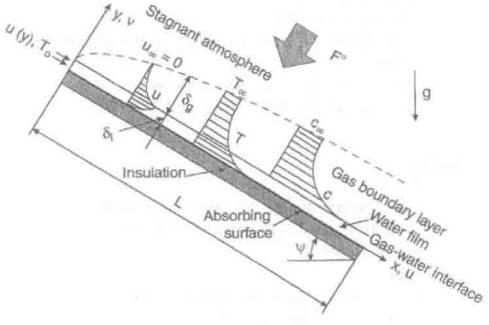

Fig. 1. Schematic diagram of the physical system

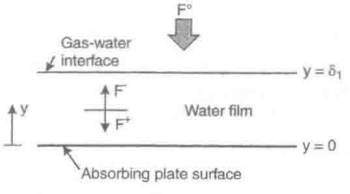

Fig. 2. Schematic of the radiation model

gas, and can be calculated from the mixing length law found by Foerthmann [9]. $Pr_{tl} = 0.9, Pr_{tg} = 0.7$ and $Sc_t = 0.7$ are the turbulent Prandtl number for water, the turbulent Prandtl number for gas and the turbulent Schmidt number for gas, respectively. The second term on the right side of Eq. (1) represents the energy transfer due to the film absorption of the solar radiation, which has been neglected in the analysis of Gandhidasan [4]. The second term on the right side of Eq. (2) represents the transport of energy due to the concentration gradient which has not been considered in the analysis of Yan and Soong [1]. The mass and momentum equations for turbulent water and gas flows are normal boundary layer equations, and would not be listed herein.

The boundary conditions for the problem are

$$x = 0 : u_l = u(y),\ T_l = T_o,\ u_g = 0,\ T_g = T_\infty,\ c = c_\infty \tag{8}$$

$$y = 0 : u_l = 0, \quad -k_l \frac{\partial T_l}{\partial y} = \int_0^{\lambda_c} \alpha^*_{w\lambda} F^+_\lambda(0)\, d\lambda \tag{9}$$

and

$$y \to \infty : u_g = 0, \quad T_g = T_\infty, \quad c = c_\infty \tag{10}$$

At the gas-water interface ($y = \delta_l$), the continuities of velocity, temperature and shear stress, and the energy balance must be met, e.g.

$$u_I = u_l = u_g \tag{11}$$

$$T_I = T_l = T_g \tag{12}$$

$$\left[(\mu_l + \rho_l \epsilon_{Ml}) \frac{\partial \mu_l}{\partial y}\right]_{I,l} = \left[(\mu_g + \rho_g \epsilon_{Mg}) \frac{\partial \mu_g}{\partial y}\right]_{I,g} \tag{13}$$

and

$$\int_{\lambda_c}^{\infty} \alpha^*_l F^0_\lambda\, d\lambda - \left[\left(k_l + \frac{\rho_l c_{pl} \epsilon_{Ml}}{Pr_{tl}}\right) \frac{\partial T_l}{\partial y}\right]_{I,l} = h_{fg} \dot{m} - \left[\left(k_g + \frac{\rho_g c_{pg} \epsilon_{Mg}}{Pr_{tg}}\right) \frac{\partial T_g}{\partial y}\right]_{I,g} \tag{14}$$

By considering the solubility of air in the water film to be negligibly small, the transverse velocity of the air-vapor mixture in the gas-water interface can be

$$v_I = -\left[\frac{D + \frac{\epsilon_{Mg}}{Sc_t}}{1 - c} \frac{\partial c}{\partial y}\right]_{I,g} \tag{15}$$

Assuming the gas-water interface at saturation pressure p_{vI}, the interfacial mass fraction of water vapor can be evaluated by [3]

$$c_I = \frac{p_{vI}}{(p_g - p_{vI}) \frac{M_g}{M_v} + p_{vI}} \tag{16}$$

The variations of thermodynamic and transport properties with temperature and mixture composition in this study are considered. The transport properties for air used in the present study were taken from Zhong et al. [10]. Other pure property data and the mixture properties were gained from Reid et al. [11]. The volumetric radiation property of water and the radiation surface properties of water and the plate were taken from available literature sources [12, 13]. The cutoff wavelength for water is assumed to be $\lambda_c = 2.5\,\mu m$.

3 Solution method

A control-volume finite-difference procedure [14] was used to solve the coupling equations. A fully implicit numerical scheme was employed. The convective term was approximated by power-law form, and a total of 151×1202 grids was used across the water film and gas layer thickness. The system of algebraic discretization equations obtained for water and gas regions was solved through the line-by-line application of the tri-diagonal matrix algorithm. It is noted that at the gas-water interface the matching discretization equations were set up by making momentum and energy balances. To avoid the divergence of iterations, the time interval in the discretization equations for unsteady problems was chosen as a specific under-relaxation factor to solve our steady problem. The total radiation fluxes were evaluated numerically using a spectral-band model, and a total of 21 spectral bands was used.

4 Results and discussion

The system parameters are important to the system analysis. Considering the climate condition which changes with season, geographic position, solar time and etc [15], we chose the parameters ranges in this study as: $30^\circ \le \psi \le 60^\circ, 0 \le F^o \le 1190\ W/m^2, 5 \times 10^{-4} \le \delta_l \le 1.5 \times 10^{-3}\ m, 288 \le T_\infty \le 298\ K, 0.003 \le c_\infty \le 0.014$ and $L = 1.5\ m$. The inlet water temperature, T_o, was set on 293.15 K.

Figures 3 to 6 show the variations of the absorbing plate surface temperature, T_w, and the gas-water interfacial

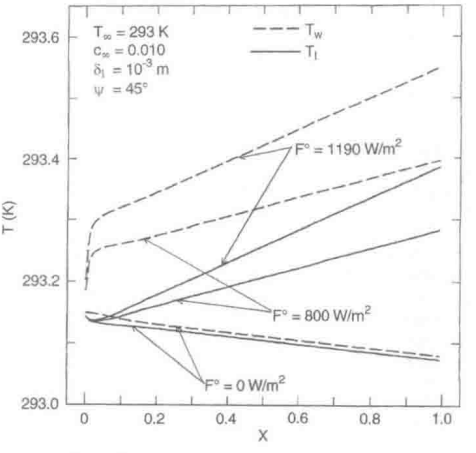

Fig. 3. Effects of F^o on T_w and T_I

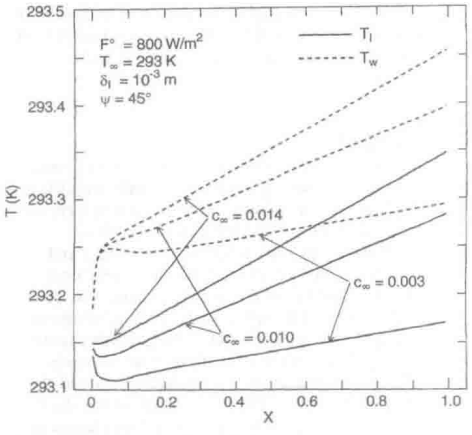

Fig. 4. Effects of c_{∞} on T_w and T_l

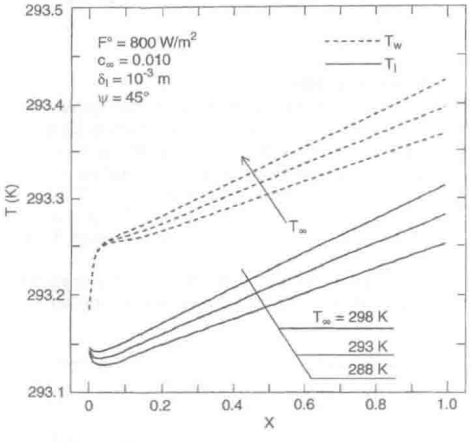

Fig. 5. Effects of T_{∞} on T_w and T_l

temperature, T_l, with dimensionless coordinate, X, under the various conditions of the solar incident flux, F^o, the mass fraction of water vapour in the ambient atmosphere, c_{∞}, the atmospheric temperature, T_{∞}, and the tilt angle, ψ, respectively. As expected, continuous radiant heating raises both T_w and T_l along the flow direction except in the neighborhood of $X = 0$, in which the high evaporation rate and heat transfer coefficient bring about a drop of the interfacial temperature. The tendency of the drop in T_l depends on the ambient temperature and humidity as well as the water flow turbulence. Any decrease of c_{∞}, or T_{∞} will lead to increase the magnitude of the drop in T_l, which has been shown in Figs. 4 and 5. This should be attributed to that the decrease of c_{∞} or T_{∞} enhances the heat

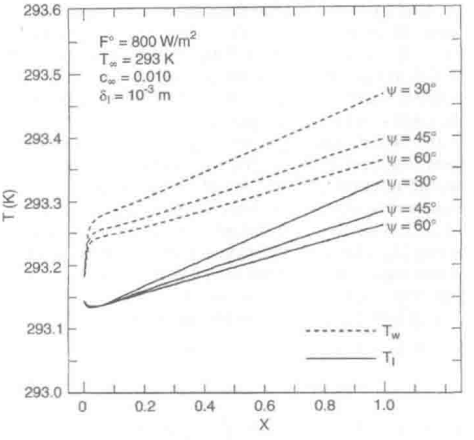

Fig. 6. Effects of ψ on T_w and T_l

transmission from the gas-water interface to the gas boundary layer. For $F^o = 0$, T_l and T_w have no way of rising but dropping down along the flow direction as the evaporation, and the sensible heat transfer between the water film and the gas layer transport the energy from the water film. At the position near the inlet ($X = 0$), the plate surface temperature, T_w, rises dramatically to a specific value, which depends on the magnitude of solar incident flux (Fig. 3), and the plate tilt angle (Fig. 6), and then rises along the flow direction at a lower rate. But if the heat transfer is high enough, T_w after reaching the specific value will slightly drop for a while, and then gradually rise somewhat, which is evidenced in Fig. 4 for $c_{\infty} = 0.003$. In latter developed region of the boundary layer the variations of T_w and T_l with X are almost linear. This indicates that the magnitude of heat and mass transfer remains constant in the developed region. An increase in F^o, c_{∞} or T_{∞} will certainly result in the rise of T_l and T_w. The tilt angle, ψ, represents the influence of the gravitational force. With the increase of ψ, the gravitational force plays more roles in fluid dynamics, which increases flow velocity and the heat capacity of the film flow so that the heat and mass transfer would be enhanced and the magnitude of the temperature rise of the water film would be limited.

Figure 7 demonstrates the axial distributions of the mean x-direction velocity and mean temperature of the water film, u_m and T_m, the plate surface temperature, T_w, and the gas-water interfacial temperature, T_I. u_m first dramatically drops from a initial value of 1.186 m/s to its lowest value of 1.182 m/s by the action of interfacial viscous frictional force, and then rises at variable rates by the actions of the gravitational and inertial forces. In the region near the inlet, the water flow needs to spend some of its momentum to bring about the stagnant atmosphere flowing with it, which reduces the water flow velocity. With the development of the gas boundary layer the interfacial shear stress is gradually reduced so that the velocity of the

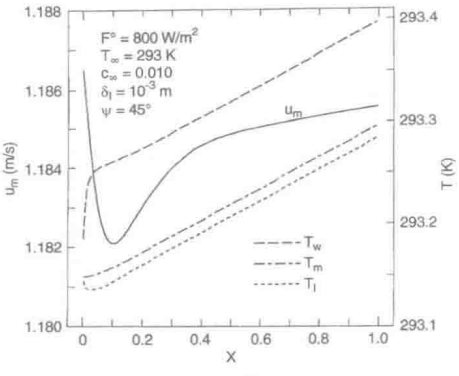

Fig. 7. Axial distributions of u_m, T_m, T_w and T_l on specific conditions

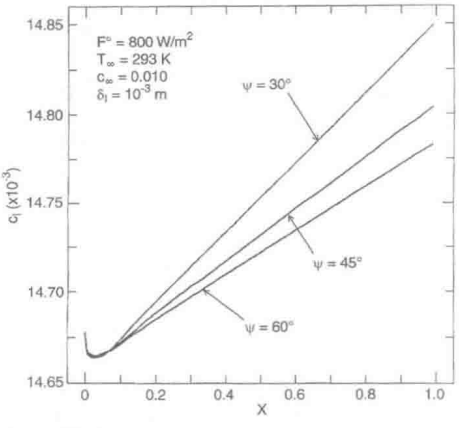

Fig. 8. Effect of ψ on c_l

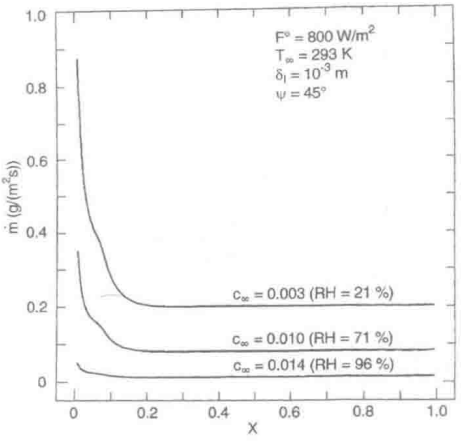

Fig. 9. Effect of c_∞ on $\dot{m}$

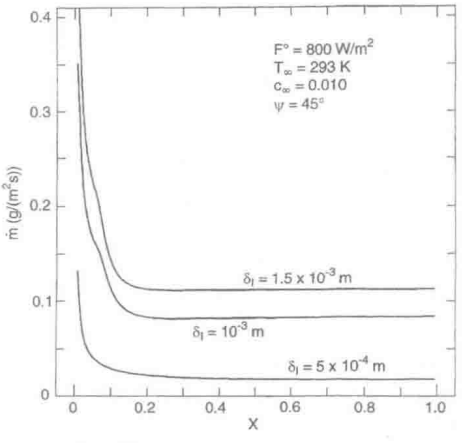

Fig. 10. Effect of δ_l on $\dot{m}$

water flow could be recovered as much as 78.7% of its lost at the outlet of water flow. T_m is more closed to T_l, which indicates the temperature in the water film with turbulent flow (Re = 4702) approximates to a uniform value except its linear distribution in the viscous sublayer near the plate surface, which is evidenced in our investigation.

The variations of interfacial mass fraction of water vapor, c_l, with dimensionless coordinate, X, for some tilt angles, ψ, are plotted in Fig. 8. Comparing these with the data in Fig. 6, it is clear that the tendency of the axial distribution of c_l is quite similar to that of T_l, in view of the relation of $c_l = f(T_l)$.

The mass and heat fluxes at the gas-water interface are the most dominant parameters for mass and heat transfer from the water film to the gas layer. The total interfacial heat flux, q_x, consists of two parts that one is sensible heat flux, q_s, and the other is latent heat flux, q_l. The variations of interfacial mass flux, $\dot{m}$, with X for various parameters of c_∞, and δ_l are shown in Figs. 9 and 10. The interfacial mass flux decreases sharply in the range of $X < 0.2$, and beyond $X = 0.2$, it approaches to a certain value according to c_∞, and δ_l. The absolute value of $\dot{m}$ and its variation for each parameter would be mainly dependent on the concentration gradient in the gas boundary layer and the flow turbulence. The lower atmospheric humidity ($c_\infty = 0.003$, RH = 21%) causes a higher concentration gradient in the gas boundary layer so that $\dot{m}$ in the region

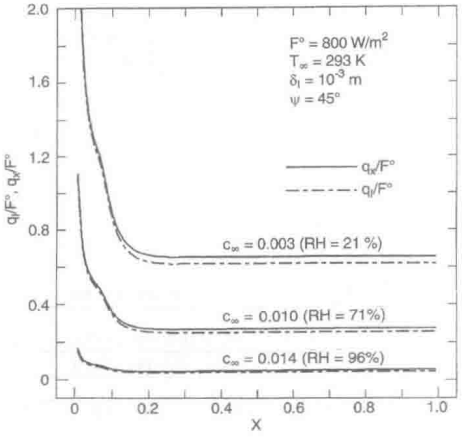

Fig. 11. Effects of c_∞ on q_l/F^o and q_x/F^o

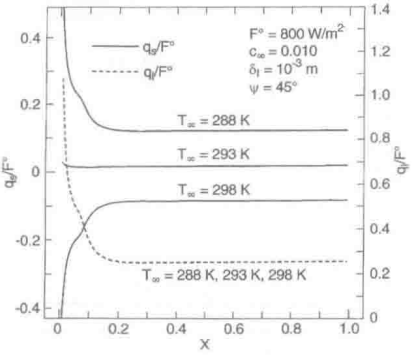

Fig. 12. Effects of T_∞ on q_s/F^o and q_l/F^o

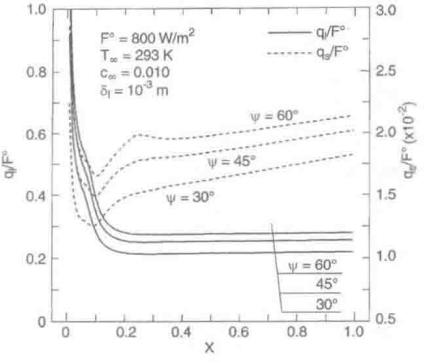

Fig. 13. Effects of ψ on q_s/F^o and q_l/F^o

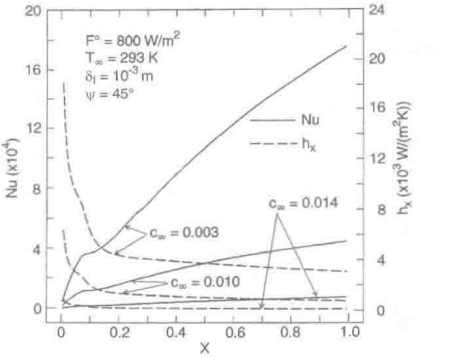

Fig. 14. Effects of c_∞ on h_x and Nu

of $X > 0.2$ could reach as high as 0.203 g/(m^{2}s). However under the condition of $c_\infty = 0.014$ (RH = 96%), $\dot{m}$ is only about 0.015 g/(m^{2}s) (Fig. 9). The increase in δ_l raises the interfacial velocity so that the mass transfer is enhanced and $\dot{m}$ can arrive at a higher value (see Fig. 10).

Figures 11 to 13 present the variations of dimensionless heat flux q_s/F^o, q_l/F^o, and q_x/F^o with X for various parameters of c_∞, T_∞, and ψ. The tendency of the variation of q_l/F^o or q_x/F^o with X in Fig. 11 is associated with that of $\dot{m}$ in Fig. 9, since q_l or q_x is a function of $\dot{m}$. Figure 11 reveals that the ambient humidity exerts an intense influence on interfacial heat flux, q_x or q_l. When the mass fraction of water vapor in the ambient atmosphere, c_∞, is 0.014 (RH = 96%), the heat loss rate, q_x/F^o, from the water film is only about 6% of the incident radiative flux in the region of $X > 0.2$. However as c_∞ reduces to 0.003 (RH = 21%), q_x/F^o reaches a very high value of around 66% . From the results of Fig. 12, it is noticed that the ambient temperature, T_∞, dramatically affects the heat loss rate q_s/F^o although its influence on q_l/F^o is very small. Under the condition of $T_\infty \approx T_o$, q_s/F^o is only about 2% in the developed region. However as T_∞ is at 288 K which is about 5 K less than T_o, q_s/F^o can reach a value of around 12% . On the other hand, if T_∞ is at 298 K which is about 5 K higher that T_o, the value of q_s/F^o approaches to about −8%, which means that the sensible heat is transferred from the gas layer to the water film. The value of q_s/F^o in Fig. 13 first drops dramatically to a minimum at about $X = 0.1$, and then rises gradually along the flow direction except the data for $\psi = 60°$, which is attributed to the changes in the interfacial temperature and heat transfer coefficient due to radiant heating and the axial distribution of the water flow velocity. The value of q_s/F^o for $\psi = 60°$ reaches a local maximum at about $X = 0.25$. The behavior could be

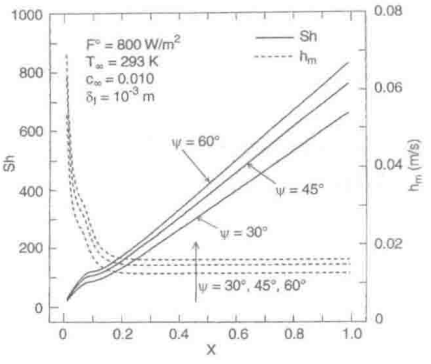

Fig. 15. Effects of ψ on h_m and Sh

explained by the fact that the dragged water flow velocity grows at the highest rate near $X = 0.25$ (reference to Fig. 7), which causes an obviously local maximum of the interfacial heat transfer coefficient. The data reveal that q_l is about 13 times greater than q_s.

The rate of heat and mass transfer can be also expressed with the heat and mass transfer coefficients or Nusselt and Sherwood numbers. The variations of Nu and h_x, as well as Sh and h_m with X for different c_∞ and ψ, are shown in Figs. 14 and 15, respectively. From the result of Fig. 14, it is obvious that the decreasing of c_∞ enhances not only the mass transfer but also the heat transfer. Figure 15 indicates that Sherwood number increases with an increase in the tilt angle, ψ. This effect of ψ could be explained by the fact that an increasing of ψ results in the increases in flow velocity and flow turbulent intensity. The values of Nu and Sh remain about constant in the neighborhood of $X = 0.1$ in Figs. 14 and 15, which would be attributed that the dragged flow velocity make the heat and mass transfer coefficients drop markedly, and means that the first derivatives of Nu and Sh with respect to X might equal to zero around $X = 0.1$.

5 Conclusions

The heat and mass transfers of a water film falling down a tilted plate with radiant heating and water evaporation have been studied numerically in this paper. The effects of various parameters on them were investigated. From the results and discussion, the following conclusions can be drawn.

It was clarified in numerical quantities that among the influential factors of heat and mass transfer, the gradients of mass fraction of water vapor and temperature between the gas-water interface and the ambient atmosphere as well as the water flow turbulence played an important role. The latent heat flux and heat transfer coefficient could be 10 to 15 times larger than the sensible heat flux and heat transfer coefficient, respectively. Although the atmospheric temperature exerted few influences on the interfacial latent heat flux, it had an obvious effect on the interfacial sensible heat flux. The magnitude of solar radiative flux incident on the gas-water interface played an important role in the change of water temperature.

References

1. **Yan WM; Soong CY** (1995) Convective heat and mass transfer along an inclined heated plate with film evaporation. Int. J. Heat Mass Transfer 38: 1261–1269
2. **Karapantios TD; Kostoglou M; Karabelas AJ** (1995) Local condensation rates of steam-air mixtures in direct contact with a falling liquid film. Int. J. Heat Mass Transfer 38: 779–794
3. **Schröppel J; Thiele F; Unterlöhner O** (1981) Mass, heat, and momentum transfer in laminar and turbulent pipe flow with vaporization of a liquid film. In: R. W. Lewis, K. Morgan and B. A. Schrefler (eds.), Numerical Methods in Thermal Problems, Vol. II, Pineridge press, Swansea, pp. 1215–1226
4. **Gandhidasan P** (1986) Heat and mass transfer in solar regenerators. In: N. P. Cheremisinoff (ed.), Handbook of Heat and Mass Transfer, Vol. 2, Gulf Publishing Company, Houston, Chapter 37
5. **Grossman G** (1986) Heat and mass transfer in film absorption. In: N. P. Cheremisinoff (ed.), Handbook of Heat and Mass Transfer, Vol. 2, Gulf Publishing Company, Houston, Chapter 6
6. **Fujita Y; Tsutui M** (1994) Evaporation heat transfer of falling films on horizontal tube (1st report). Transactions of The JSME (B) 60: 3469–3474 (in Japanese)
7. **Yih SM** (1986) Modeling heat and mass transport in falling liquid films. In: N. P. Cheremisinoff (ed.), Handbook of Heat and Mass Transfer, Vol. 2, Gulf Publishing Company, Houston, Chapter 5
8. **Yih SM; Liu JL** (1983) Prediction of heat transfer in turbulent falling liquid films with or without interfacial shear. AIChE Journal 29: 903–909
9. **Schlichting H** (1979) Boundary-layer Theory. (translated by J. Kestin), 7th edition, New York: McGraw-Hill
10. **Zhong ZY; Yang KT; Lloyd JR** (1985) Variable-property natural convection in tilted Enclosures with thermal radiation. In: R. W. Lewis and K. Morgan (eds.), Numerical Methods in Heat Transfer, Vol. III, John Wiley & Sons, Chichester, Chapter 9
11. **Reid RC; Prausnitz JM; Sherwood TK** (1977) The Properties of Gases and Liquids. 3rd edition, New York: McGraw-Hill
12. **Eckert ERG; Drake R M., Jr** (1972) Analysis of Heat and Mass Transfer. Tokyo: McGraw-Hill Kogakusha
13. **Brewster MQ** (1992) Thermal Radiative Transfer and Properties. New York: John Wiley & Sons
14. **Patankar SV** (1980) Numerical Heat Transfer and Fluid Flow. New York: Hemisphere/McGraw-Hill
15. **Japanese National Astronomical Observatory** (ed.) Chronological Scientific Tables. Tokyo: Mayuzen Co., Ltd. 1994 (in Japanese)